Coupled chemical-equilibrium/transport model calculations of soil trace-metal leaching as influenced by interactive effects of dissolved organic matter, pH, and electrolyte conditions

Dean Hesterberg[a], J. Bril[b], and P. A. C. Raats[b]

[a]Department of Soil Science, North Carolina State University, Box 7619, Raleigh, NC 27695

[b]Institute for Soil Fertility Research (IB-DLO), P.O. Box 30003, 9750 RA, Haren, Netherlands

Abstract
To better understand possible effects of soil amendments on trace-metal leaching, coupled thermodynamic and solute transport models were used to compute metal leaching from a model soil column following surface-applied treatments of $CaCO_3$, $CaSO_4$, or KCl. The thermodynamic model accounted for interactive chemical effects on metal solubility and could reasonably predict dissolved Zn and Cd concentrations measured in soil solution samples collected from a manured field soil. In the coupled chemical-equilibrium/transport model, natural variations in the concentration of a dissolved organic carbon (DOC) complexer were controlled by a Ca-DOC precipitate. Results showed that after introducing a soil amendment, a wave of increased or decreased ionic strength solution discharged from the column caused a corresponding wave of metal discharge.

1. INTRODUCTION

Field and column studies have addressed the potential environmental problem of trace metal leaching in soils [1-2]. Metal solubility was often found to increase with decreasing pH, increasing solubility of complexing inorganic or organic ligands (e.g., fulvic acid), and increasing soil-solution ionic strength [2-5]. A recent field study [6] showed that applying cattle-manure slurry to a loamy-sand soil affected Zn and Cd solubilities. Because manuring also affected soil-solution macrochemistry, we previously developed a thermodynamic model [7] to try to predict spatial and temporal variations in field measurements of dissolved trace metals. The model accounted for combined effects of macrochemical parameters such as pH, ion concentrations, and dissolved organic carbon (DOC) complexer.

To illustrate the field data serving as the basis for model development, Fig. 1 gives an example of macrochemical and trace-metal solubility trends observed over time in a manured soil. In samples collected about 50 days after manuring (i.e., at 109 days in Fig. 1), dissolved Ca and Zn were about 12-fold and 6-fold (respectively) greater than prior to manuring, while pH and DOC decreased. Similar to Ca and Zn, measured concentrations of K, Mg, Na, Cd, and Cl, and electrical conductivity were increased after manuring (data not shown). The increased soil-solution ionic strength at 109 days was attributed to inputs of basic cations and anions contained in the animal manure [8]. At 240 days after manuring, most soil-solution conditions that were changed by manuring were reverted back to conditions more closely resembling those before manuring (Fig. 1). It appeared that ions added with the manure

dissipated by leaching through the soil profile (see data in [7]). Close inspection of the data in Fig. 1 also indicates that dissolved Zn was not strictly dependent on any single macrochemical parameter shown, but was likely influenced by combined effects of macrochemical components.
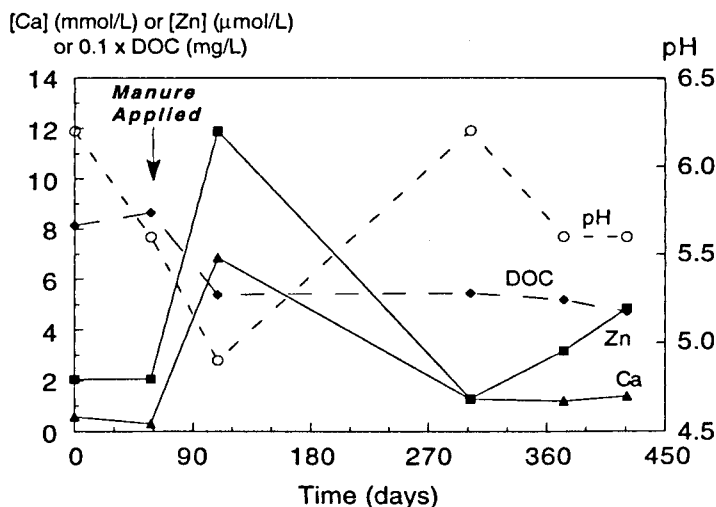

Figure 1. Total dissolved concentrations of calcium, zinc, and dissolved organic carbon ([Ca], [Zn], and DOC) and pH measured over time in soil solution samples extracted from the top 20 cm of a loamy-sand field soil that received a cattle-manure slurry application of 25 Mg/ha following the second sampling. (Data are from references [6] and [7] for the 160 Mg/ha historical manuring treatment).

Because variations in soil-solution macrochemistry affect trace metal solubility, the objective of the present study was to couple the previously developed thermodynamic model [7] with a solute transport model to illustrate how soil amendments such as calcite, gypsum, or KCl-fertilizer might affect short-term soil Zn and Cd leaching. With the thermodynamic model accounting for multiple chemical interactions, we computed discharge of Zn, Cd, and macrochemical components from a homogeneous model soil column representing the uniform topsoil of the experimental field studied previously [6].

2. COUPLED CHEMICAL-EQUILIBRIUM/TRANSPORT MODEL

2.1. The chemical-equilibrium model

Given inputs of soil-solution macrochemistry (e.g., major cation and anion concentrations, and pH) and soil properties (e.g., acid-extractable trace-metal and organic C contents), the model accounted for dissolved inorganic aqueous complexes and competitive cation complexation by a DOC complexer and an organic matter exchanger phase.

The thermodynamic model developed for the chemical-equilibrium program CHARON [9] and used to predict trace-metal solubilities was described in detail elsewhere [7]. Basically, thermodynamic parameters for all inorganic interactions (e.g., aqueous complex formation) were derived from literature data. Both DOC complexer and solid organic matter exchanger components were given pH-dependent, competitive cation complexation constants based on conditional, average equilibrium quotients for 1:1 metal:fulvic acid complexes normalized to a complexing capacity of 2 mol/kg-C [4,7]. Complexation parameters were not calibrated based on the field data, but were derived strictly from the literature data and the assumption that the solid organic matter had the same complexing capacity and affinity for metals as the DOC complexer. Other relevant assumptions used to develop the thermodynamic model were 1) the soil solution was in a state of chemical equilibrium at each sampling time, 2) the soil was sufficiently aerated that chemical components modeled remained in their oxidation state common to well-aerated soils, 3) organic matter was the dominant exchanger phase for metals, and 4) acid-extractable soil trace metals equaled exchangeable metals [7].

Figure 2 shows a comparison of dissolved trace-metal concentrations predicted by the model and concentrations measured in field-soil samples. Predicted dissolved Zn and Cd concentrations deviated from measured concentrations on the average 1.4- and 2-fold (respectively) for 120- and 34-fold measured concentration ranges [7]. Because the model accounted for much of the variation in dissolved Zn and Cd for a range of soil solution conditions, we expect that in the present study, modeling results give insights to general trends in Zn and Cd leaching after applying soil amendments.
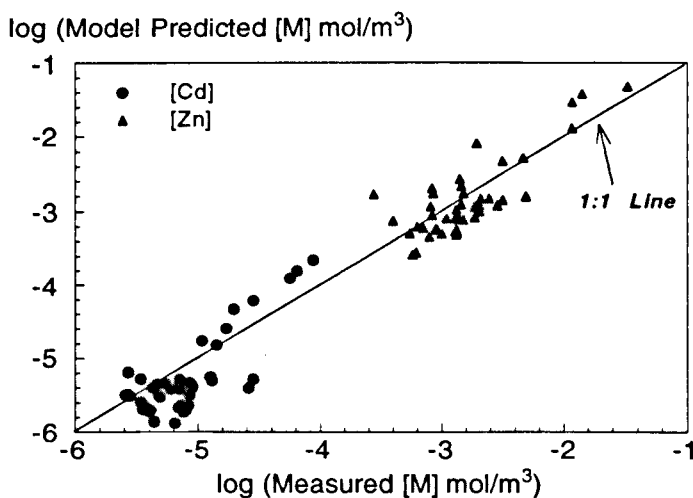

Figure 2. Comparison of model-predicted and measured dissolved Zn and Cd concentrations ([M] is total dissolved metal concentration) in samples collected over time from three field plots and four soil depth intervals (data from [7]). Soil solutions ranged from pH 4.5 to 6.7, had electrical conductivities between 15 and 508 mS/m, and contained between 30 and 260 mg DOC/L.

To facilitate interpretation of data from coupled thermodynamic/transport simulations, the original model components Mg, Na, NH_4, NO_3, PO_4, Al, and Cu were excluded for the

present study. The principal model components included were H, OH, Ca, K, Zn, Cd, SO_4, Cl, CO_3, DOC complexer, and the exchanger phase; with 50 chemical species considered. We expected that elimination of the selected components would not significantly affect the modeling trends for the following reasons: 1) [Ca] was on the average more than 3-fold greater than [Mg] in the soil solutions used to develop the model, and stability constants for Ca^{2+}-organic matter complexes were about 1.2 log units greater than stability constants for Mg^{2+}-organic matter complexes [7], indicating that Ca^{2+} was the dominant divalent cation competing with trace metals for the exchanger phase and soluble complexer; 2) in the original model [7], the stabilities of complexes involving organic matter were equivalent for monovalent cations or monovalent anions, thus Na^+ and NH_4^+ behaved like K^+ while NO_3^- behaved like Cl^-; 3) modeling results [7] indicated that inorganic complexes involving trace metals were usually minor compared with dissolved organic matter complexes, and 4) [PO_4], [Al], and [Cu] occurred in low solution concentrations, and, for example, except in cases of low pH and low DOC, the model predicted that the fraction of DOC complexed with Al^{3+} or Cu^{2+} was less than 0.01. Although we eliminated components, interactions between the remaining components (e.g., soluble organic and inorganic complexation and exchange reactions [7]) were considered in the coupled equilibrium/transport model.

Variations in DOC observed in the field were incorporated into the model by assuming that a Ca-DOC precipitate controlled DOC-complexer concentrations (see e.g., [10] for a description of humic substances precipitation). Note that this precipitation reaction was included in addition to other complexation reactions involving DOC. The model DOC complexer was a dibasic acid, H_2DOC(aq), with proton dissociation constants log K_{A1} = -4.3 and log K_{A2} = -9.3, which were derived from proton titration experiments on a loamy-sand soil considered similar to the modeled experimental field soil (Bril, unpublished data). Note that compared with the original thermodynamic model, two dissociation reactions were included in the present model, and log K_{A1} is more negative than in the original model (log K_A = -3.8 in [7]). Field-soil solution data [7] showed a correlation between [$HDOC^-$(aq)] and [Ca^{2+}(aq)], the aqueous concentrations of monoprotonated DOC complexer and free ionic Ca species (Fig. 3). It was assumed that the total DOC complexer concentration equaled 2 mol/kg-DOC [7]. Corrections for aqueous Ca-DOC complexes were made, while aqueous inorganic Ca complexes and other DOC complexes were considered to be insignificant, as suggested by previous modeling results [7].

To determine from the field data a conditional solubility product constant (in terms of concentrations) ($^cK_{so}$) for the Ca-DOC solid, consider the dissolution reaction

$$Ca(HDOC)_2(s) \rightleftharpoons Ca^{2+}(aq) + 2\ HDOC^-(aq) \tag{1},$$

where $^cK_{so}$ can be written as

$$\log\ ^cK_{so} = \log\ [Ca^{2+}(aq)] + 2 \log\ [HDOC^-(aq)] \tag{2}$$

or

$$\log\ [HDOC^-(aq)] = -0.5 \log\ [Ca^{2+}(aq)] + 0.5 \log\ ^cK_{so} \tag{3},$$

when solid-phase activity is assumed to be unity. A linear regression between [$HDOC^-$(aq)] and [Ca^{2+}(aq)] yielded (Fig. 3 - "Best Fit")

$$\log\ [HDOC^-(aq)] = -0.56 \log\ [Ca^{2+}(aq)] - 5.6 \tag{4},$$

which had an r^2 of 0.71 and standard deviations of 0.06 and 0.2 for the slope and intercept. By setting the regression slope to 0.5 to obtain a solid-phase stoichiometry consistent with Eq. (3), the resulting equation was (Fig. 3 - "Model Used")

$$\log [HDOC^-(aq)] = - 0.5 \log [Ca^{2+}(aq)] - 5.51 \tag{5}.$$

log ([HDOC⁻] mol/L)

log ([Ca²⁺] mol/L)
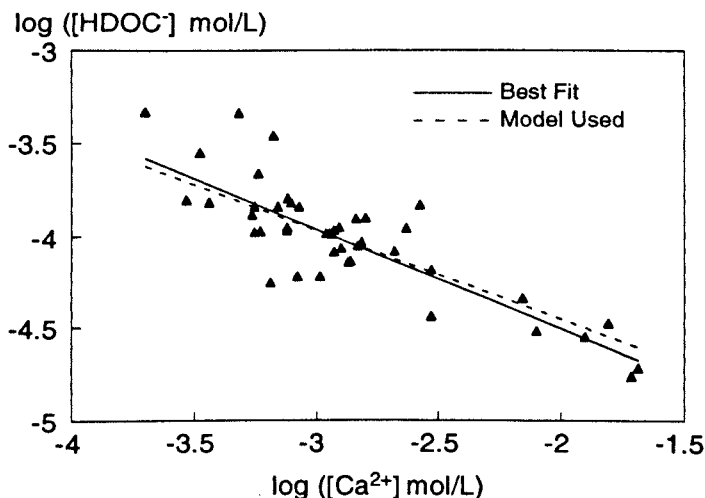
Figure 3. Relationship between concentrations of monoprotonated dissolved organic carbon complexer used in the model ([HDOC⁻(aq)]) and dissolved free-ionic calcium ([Ca²⁺(aq)]) derived from field-soil solution measurements.

Comparing Eqs. (3) and (5) shows that log $^cK_{so}$ derived from the field data is -11.02. Using the average ionic strength (I) determined from soil solution electrical conductivities (EC) and the relationship between I and EC found by Griffin and Jurinak [11], the Davies equation [12] was used to compute an average activity correction for Ca²⁺ only. This correction yielded the solubility product constant -11.36, which was used in the model for the solid phase $Ca(HDOC)_2(s)$. By including in the model soil an amount of $Ca(HDOC)_2(s)$ in excess of what would be dissolved during the transport simulations, [HDOC⁻(aq)] varied as a function of soil solution composition. This solid phase was treated independently from the organic matter exchanger phase.

2.2. The transport model

Model calculations for steady flow in saturated soil simulated solute discharge from a 1 m x 1 m x 0.4 m homogeneous soil column (Fig. 4), representing the top 0.4 m of a loamy-sand field soil in the Netherlands. The column was divided into twenty 2-cm thick layers, each treated as a separate system for calculating chemical equilibrium each time step. The acid-extractable Zn and Cd concentrations and other properties given in Fig. 4 are based on field data [7]. The cation complexing capacity of the organic matter exchanger phase was 0.044

mol/kg-soil (2 mol/kg-C), which is within the range (0.036 - 0.083 mol_c/kg) of cation exchange capacities reported [13] for sandy soils in the Netherlands.

Simulated Soil Solution
and
$CaSO_4$, KCl, or $CaCO_3$ Treatment

$1 m^2$ surface

40 cm

Model Soil Column

Total Zn = 12 mg/kg
Total Cd = 0.15 mg/kg
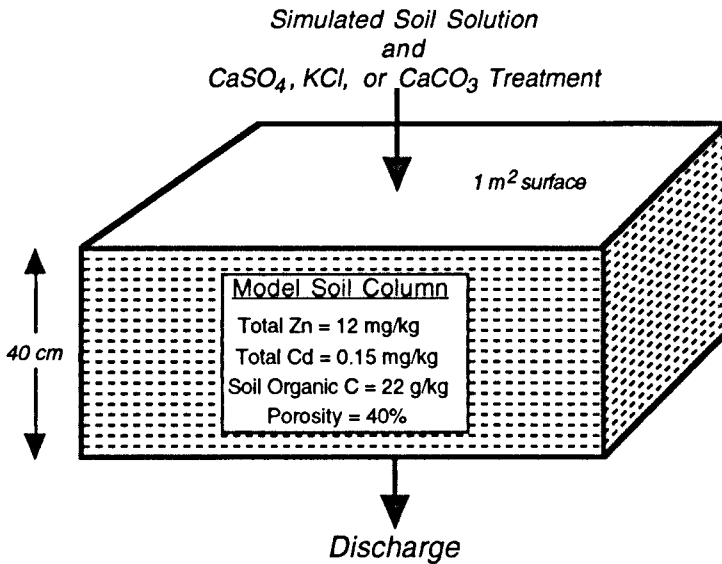Soil Organic C = 22 g/kg
Porosity = 40%

Discharge

Figure 4. Schematic of the model soil column, including some initial soil conditions.

To compute dissolved chemical-component transport, the chemical equilibrium model was coupled to CHARON's transport algorithm [9], which is based on the one-dimensional convection-dispersion equation [14] describing solute flux as a sum of convective and dispersive fluxes. The average pore water velocity (v_o) in our model was 0.625 cm/day. The dispersion coefficient (D) in the convection-dispersion equation is expressed as a product of dispersion length (λ) and v_o. In most simulations, λ = 1.2 cm (numerical dispersion only); while in one KCl-treatment case, the overall λ, including the contribution of numerical dispersion to D (see [14]), was 5 cm. Time steps of either 0.5 day (for λ = 1.2 cm) or 0.25 day (for λ = 5 cm) were used.

In the computer simulations, the initial soil saturating solution and the solution continually introduced at the top of the column had a chemical composition approximately equal to the solution composition measured in the field study before a manure treatment [6,7], but adjusted to pH 5. Total dissolved concentrations of Ca, K, SO_4, Cl, CO_3 and DOC complexer equaled 0.51, 0.90, 0.30, 1.16, 0.11, and 0.18 mol/m^3, while Zn and Cd concentrations in the introduced solution were essentially nil (10^{-8} mol/m^3). The $CO_2(g)$ partial pressure (P_{CO_2}) was fixed at 0.003 atm in each soil layer. After 0.3 full-column pore volumes (PVs) of solution throughput, a single pulse of either 0.1 moles of $CaCO_3$ or $CaSO_4$, or 0.2 moles of KCl was added to the aqueous phase at the column's top surface, and subsequent ion discharge from the bottom of the column was followed. A portion of the simulated $CaCO_3$ treatment precipitated as calcite in the top column segment, then redissolved during the course of about 0.15 column PVs of flow.

3. MODELING RESULTS AND DISCUSSION

Figure 5 shows model-predicted Ca discharge rates and solution pH, and Fig. 6 shows corresponding model-predicted Cd and Zn discharge rates following $CaCO_3$, $CaSO_4$ or KCl treatments applied to the model soil column. Relative discharge rates of K, SO_4, and Cl between the various treatments (data not shown) were qualitatively the same as the Ca discharge (Fig. 5). Because these were the more prevalent aqueous components in addition to Ca, ionic strength followed the same trends as Ca in the discharged solutions.
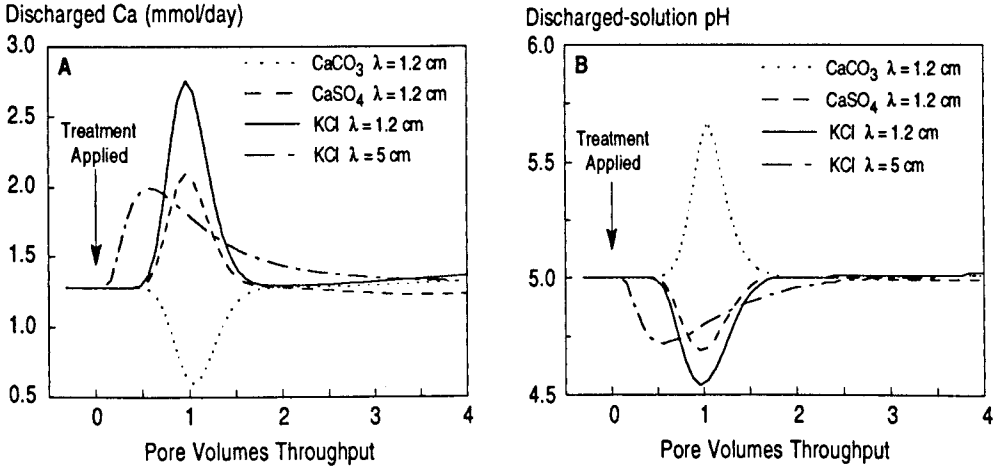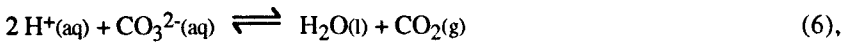
Discharged Ca (mmol/day)   Discharged-solution pH

Figure 5. Model-predicted calcium discharge (A) and solution pH (B) at the bottom of the model soil column after surface applying 0.1 moles of $CaCO_3$ or $CaSO_4$, or 0.2 moles of KCl (λ is dispersion length).

Calcium discharge and pH showed opposite trends for a given treatment (Fig. 5). For $CaSO_4$ or KCl treatments, protons displaced from the exchanger phase decreased pH. For the $CaCO_3$ treatment under conditions of fixed P_{CO2}, protons were consumed by the reaction

$$2\,H^+_{(aq)} + CO_3^{2-}_{(aq)} \rightleftharpoons H_2O_{(l)} + CO_{2(g)} \qquad (6),$$

which raised pH. Replacement of exchanger-phase protons with Ca^{2+}, K^+, Zn^{2+}, and Cd^{2+} decreased dissolved concentrations of these species and the solution ionic strength, as indicated by the negative peaks in Figs. 5A and 6.

In cases of low solute dispersion ($\lambda = 1.2$ cm), positive or negative ionic-strength peaks occurred near 1 PV of solution throughput following the treatment (indicated by data in Fig. 5A). For a KCl treatment and $\lambda = 5$ cm, the ionic-strength wave broadened and the peak flux shifted to an earlier time (Fig. 5). Although non-linear, multiple-component exchange processes occurred, peaks near 1 PV (for $\lambda = 1.2$ cm) suggested that an ionic-strength wave passing through the column behaved conservatively. In fact, theoretical 1-dimensional transport calculations [15] indicated that when several solute species compete for a fixed number of adsorption sites in the absence of precipitation/dissolution reactions, the sum of ions

moving through the system behaves like an ideal tracer. Since our model complied with mass balance constraints and included an exchanger phase of fixed cation complexing capacity, the model-predicted ionic strength wave discharged from the column near 1 PV (Fig. 5) was qualitatively consistent with the theoretical calculations, but was also affected by precipitation/dissolution and $CO_2(g)$ volatilization reactions.
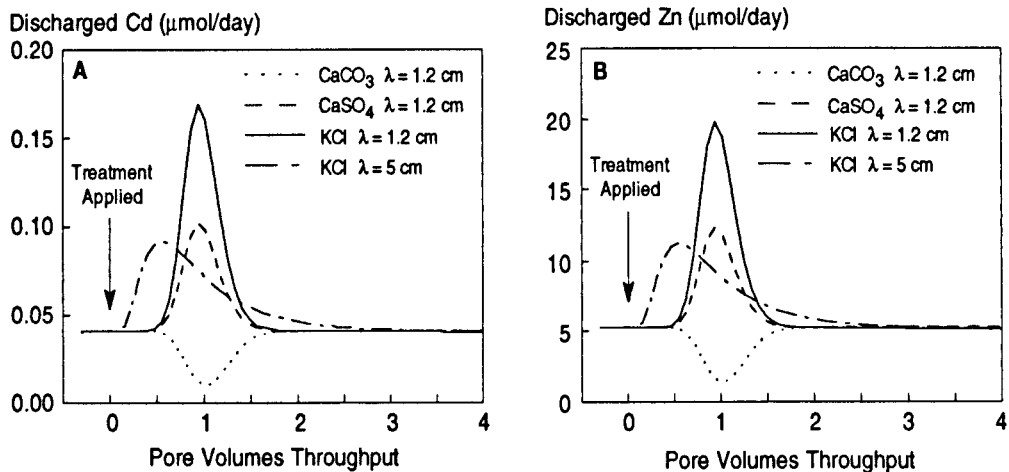

Figure 6. Model-predicted discharge of cadmium (A) and zinc (B) from the model soil column for the treatments described in Fig. 5.

To elucidate effects of precipitation/dissolution or volatilization reactions on ion discharge following a surface-applied treatment, we approximated the absolute value of the total discharged cationic- and anionic-component charge relative to the background solution charge. This approximation was made by first numerically integrating each aqueous component discharge curve (as in Fig. 5A) relative to the background solution baseline, then multiplying the integrated component discharge by the absolute value of the component's charge, and finally summing over all model components. (Note that this calculation did not differentiate chemical species charge, but rather the charge attributable to components - Ca, K, Cl, etc.). For each of the two KCl-treatments ($\lambda = 1.2$ or 5 cm), this sum of charge was 0.46 moles, which was slightly greater than the KCl input charge of 0.4 moles (0.2 moles each of K+ and Cl-). Compared with the KCl treatment, the $CaCO_3$ treatment yielded a sum of dicharged component charge (-0.24 moles) that was much decreased because of volatilization by reaction (6) and precipitation by reaction (1); while the $CaSO_4$ treatment yielded a sum of charge (0.22 moles) that was somewhat reduced because of precipitation by reaction (1).

Model-predicted discharges of Cd and Zn were qualitatively similar to Ca and K discharges for the various treatments (Fig. 6). The Cd flux was roughly 100-fold lower than the Zn flux, consistent with a lower solubility and soil concentration of Cd (Figs. 2 and 4) (Zn and Cd had similar affinities for the exchanger phase and DOC complexer [7]). Although no trace metals were added at the top of the soil column, the ionic strength wave moving through the column induced discharge of resident metals from the bottom of the column. This result was consistent with field data suggesting that metal solubility increased with increasing ionic strength as well

as with decreasing pH and increasing DOC (see Fig. 1 and [7]). Comparing the two KCl treatments, the sum of model-predicted Zn or Cd discharge was about 15% less when $\lambda = 5$ cm.

Model-predicted discharges of DOC and DOC-complexed Zn (Fig. 7) were qualitatively similar to each other but opposite to the Ca discharge (Fig. 5A), consistent with Eqs. (3) and (5). Minimum DOC fluxes (Fig. 7A) were not as sharp as maximum Ca fluxes, primarily because log [HDOC^-] was about proportional to 0.5 log [Ca^{2+}] as indicated by Eq. (5).
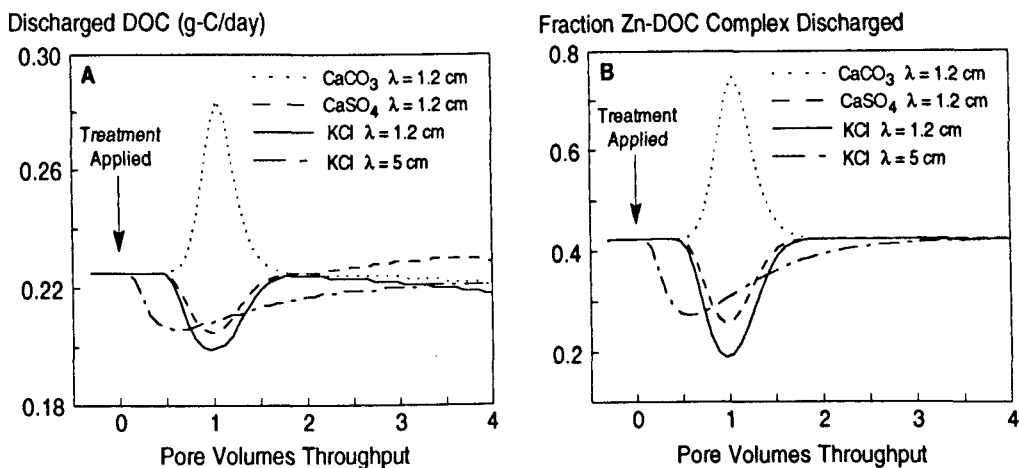

Figure 7. Model-predicted discharge of dissolved organic carbon (DOC) (A) and fraction of total discharged Zn complexed with DOC (B) for the treatments described in Fig. 5.

The model-predicted fraction of total discharged Zn that was complexed with DOC (Fig. 7B) increased as the ratio of DOC to dissolved Zn increased. Thus, for the $CaCO_3$ treatment, the minimum Zn flux near 1 PV (Fig. 6B) corresponded to a maximum DOC flux (Fig. 7A) and maximum fraction (75%) of Zn complexed with DOC (Fig. 7B). Conversely, for the maximum Zn fluxes following the $CaSO_4$ and KCl treatments, the Zn discharged was predicted to be primarily Zn^{2+} (free ionic). Model-predicted fractions of free-ionic or DOC-complexed Cd (data not shown) were essentially the same as for Zn.

Although the hypothetical treatments used in the modeling study were different than the manure treatment applied in the field, results from both studies were similar. A comparison of modeling results for the KCl and $CaSO_4$ treatments with the field data in Fig. 1 shows that under maximum solution ionic strength conditions (e.g., maximum [Ca] in simulated column-discharge solution and in field soil-solution samples), dissolved (or discharged) Zn was increased while pH and DOC were both decreased (compare Fig. 1, 60 to 300 days, with Figs 5, 6B, and 7A). Dissolved concentrations of modeled chemical components were also within the range of field-measured concentrations. For example, the simulated KCl treatment yielded a model solution exiting the column at 1PV with the following composition: pH 4.7, 1.1 mmol Ca/L, 2.7 mmol K/L, 7.9 μmol Zn/L, 0.068 μmol Cd/L, 80 mg DOC/L, 2.3 mmol Cl/L, 1.2 mmol SO_4/L, and 0.106 mmol CO_3/L. Field data presented in Figs 1 and 2 and in [7]

indicated that these relative concentrations of modeled components are quantitatively reasonable.

4. CONCLUSIONS

Coupled chemical-equilibrium/transport model calculations accounting for multiple soil-chemical interactions suggested that Zn and Cd discharge rates from a model soil column were related to the discharge of macrochemical ions following surface-applied soil amendments other than trace metals. Maximum or minimum metal discharges predicted by the model depended on the type of amendment and hydrodynamic dispersion, with KCl and $CaSO_4$ amendments increasing metal discharge primarily because of increased ionic strength and decreased pH; and $CaCO_3$ decreasing metal discharge because of decreased ionic strength and increased pH. Model-predicted metal speciation between free-ionic and DOC-complexed metal depended on the ratio of DOC to dissolved metal concentration. The modeling results presented are useful for designing short-term experiments for testing the impact of various soil amendments on trace-metal leaching rates.

5. ACKNOWLEDGMENTS

6. REFERENCES

1   R. H. Dowdy, J. J. Latterell, T. D. Hinesly, R. B. Grossman, and D. L. Sullivan, J. Environ. Qual., 20 (1991) 119.
2   M. Boyle and W. H. Fuller, J. Environ. Qual., 16 (1987) 357.
3   C. Amrhein, J. E. Strong, and P. A. Mosher, Environ. Sci. Technol., 26 (1992) 703.
4   J. Buffle, Complexation Reactions in Aquatic Systems, Ellis Horwood Publishers, Chichester, 1988.
5   G. Sposito, The Surface Chemistry of Soils, Oxford Univ. Press, New York, 1984.
6   P. del Castilho, W. J. Chardon, and W. Salomons, J. Environ. Qual. 22 (1993) (In press).
7   D. Hesterberg, J. Bril, and P. del Castilho, J. Environ. Qual. 22 (1993) (In press).
8   J. Japenga and K. Harmsen, Netherlands J. Agricul. Sci., 38 (1990) 353.
9   N. M. de Rooij and M. P. J. M. Kroot, CHARON Manual, Delft Hydraulics, Delft, The Netherlands, 1991.
10 R. S. Swift. p. 387-408 In Aiken et al. (ed.) Humic Substances in Soil, Sediment, and Water, John Wiley and Sons, New York, 1985.
11 G. P. Griffin and J. J. Jurinak, Soil Sci., 116 (1973) 26.
12 W. L. Lindsay, Chemical Equilibria in Soils, John Wiley and Sons, New York, 1979.
13 F. A. M. de Haan, S. E. A. T. M. van der Zee, and W. H. van Riemsdijk, Netherlands J. Agricul. Sci., 35 (1987) 347.
14 M. Th. van Genuchten and P. J. Wierenga, Simulation of One-Dimensional Solute Transfer in Porous Media, New Mexico State University Agricultural Experiment Station Bulletin 628 (1974).
15 C. F. Valk and P. A. C. Raats, Lumped models of convective solute transport in heterogeneous porous media 1: One-dimensional media, Institute for Soil Fertility (IB-DLO) Report No. 262 (1992); (submitted to Water Resour. Res.).